Investigations of Energy Migration in an Organic Dendrimer Macromolecule for Sensory Signal Amplification†

Meng Guo,‡ Oleg Varnavski,‡ Aditya Narayanan,‡ Oliver Mongin,§ Jean-Pierre Majoral,*,|| Mireille Blanchard-Desce,*,§ and Theodore Goodson III*,‡

Department of Chemistry, University of Michigan, Ann Arbor, Michigan 48109, Synthèse et ElectroSynthèse Organiques (CNRS, UMR 6510), Université de Rennes 1, Institut de Chimie, Campus Scientifique de Beaulieu, Bât 10A, F-35042 Rennes Cedex, France, and Laboratoire de Chimie de Coordination, CNRS, 205 route de Narbonne, F-31077, Toulouse Cedex 4, France

Received: December 18, 2008; Revised Manuscript Received: February 25, 2009

The issue of macromolecular exciton delocalization length and fluorescence sensing of energetic materials is investigated and modeled from results of nonlinear optical and time-resolved spectroscopy. By using two- and three-photon absorption techniques the fluorescence quenching effects of an organic dendrimer for sensing TNT were carried out. The Stern−Volmer plots for the set of dendrimers were examined and a large quenching constant for the dendrimer G4 was obtained (1400 M^{-1}). The quenching constant was found to increase with the dendrimer generation number. The mechanism for the enhanced sensitivity of the dendrimer system was examined by probing the exciton dynamics with femtosecond fluorescence up-conversion. Fluorescence lifetime measurements revealed a multicomponent relaxation that varied with dendrimer generation. Fluorescence anisotropy decay measurements were used to probe the exciton migration length in these dendrimer systems and for the large structure the excitation migration area covers ∼20 units. All of these results were used in a model that describes the exciton localization length with the fluorescence quenching strength. The use of time-resolved techniques allows for a closer and more detailed description of the mechanism of sensory amplification in organic macromolecules.

1. Introduction

Energy migration in organic macromolecules is an important area of research as it relates to many applications involving optical and electronic effects.[1] For example, in the energy transfer processes which are responsible for light harvesting in macromolecules,[2,3] the issue of energy migration is of great importance in probing the efficiency and mechanism of the energy transfer processes. In the very important chemosensory applications, the issue of energy migration has also been suggested to be a dominant mechanism in the amplified sensing response of certain energetic materials.[4] For example, it has been suggested that in organic conjugated polymers, the increased conjugation length may lead to more sensitive response to energetic materials.[4−8] Indeed, the issue of localization in organic systems has been considered for many organic macromolecular systems. Mukamel et al.[9] have conducted a theoretical investigation on the process of coupled chromophore systems in organic dendrimer systems with phenyl acetylene chromophores as the basic unit, and it was found that excitons could be localized on a particular branching point.[9] Later, experiments with ultrafast laser pulses (in either fluorescence up-conversion or transient absorption) demonstrated that electronic coupling between chromophores within a macromolecular geometry such as a dendrimer could be strong.[10−16] Chernyak and Tretiak later showed theoretically how one could extend the calculation of the Hamiltonian for the strongly interacting systems beyond the Frenkel exciton limit.[17] These points are certainly critical in discussing the energy migration and exciton diffusion length in multichromophore or conjugated macromolecular systems for sensory amplification.

There have been reports of the use of steady-state measurements to probe the mechanism of energy transport in certain organic macromolecules. Here, the dependence (or independence) of the oscillator strength is used as a method to isolate the processes governed by a purely columbic (Förster) or a short-range (wave function) overlap Dexter mechanism.[18] Also, the steady-state anisotropy may be used to probe the long-lived residual anisotropy of particular systems.[19,20] This method may provide qualitative information regarding energy-migration at long times mostly by use of the residual long-lived anisotropy value. However, many of the intramolecular interactions that are important in enhancing the exciton migration rate (and subsequently the fluorescence quenching ability) are governed by fast electronic processes which can only be probed by ultrafast spectroscopic techniques. These processes affect the overall energy migration pathway in macromolecules and in chemosensory applications where they are responsible for the sensitivity and Stern−Volmer results. In our previous reports of ultrafast energy migration we have found that the specific geometry of organic dendrimers may allow for strong electronic coupling leading to an ultrafast (∼50 fs) energy transfer time.[10−15]

While there have been reports of the use of exciton migration to explain the enhanced sensitivity of amplified fluorescence quenching measurements with steady-state techniques, the detailed analysis with a specific model and with both nonlinear and time-resolved techniques in systems with defined geometry

† Part of the "George C. Schatz Festschrift".

* To whom correspondence should be addressed. E-mail: tgoodson@umich.edu, mireille.blanchard-desce@univ-rennesl.fr, and majoral@lcc-toulouse.fr.

‡ University of Michigan.

§ Université de Rennes 1, Institut de Chimie.

|| Laboratoire de Chimie de Coordination, CNRS.

10.1021/jp8112123 CCC: $40.75
Published on Web 03/24/2009

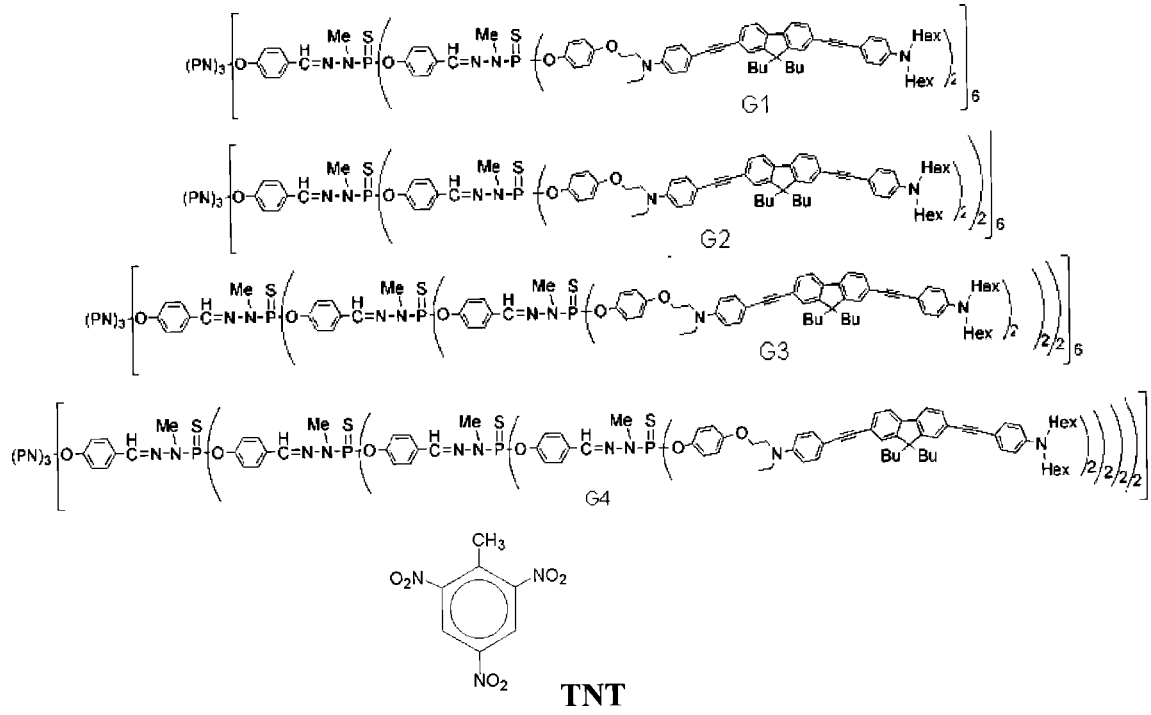

Figure 1. Chemical structure of four generation dendrimers (G1−G4) and quencher of TNT used in fluorescence quenching experiments.[23,24]

has not been reported. The quenching factor (F_0/F_q) found in Stern−Volmer plots for sensing TNT can be both modeled and related to real ultrafast and long-lived lifetimes. It can be shown that for the case of organic macromolecule of m chromophores the enhanced quenching can be related to the degree of exciton migration p (number of participating chromophores in the exciton migration) as

$$\frac{F_0}{F_q} = (1 + K_M n_a)\left(\frac{1}{1 - \left(\frac{p}{m} - 1\right)K_M n_a}\right) \quad (1)$$

where F_0 and F_q denote fluorescence intensities for nonquenched and quenched samples respectively, K_M is the association constant for macromolecule and analyte, and n_a is the number density of the analyte. Since $K_M n_a p/m \ll 1$ for trace detection with very low analyte concentration this can be approximated as:

$$\frac{F_0}{F_q} \approx 1 + \frac{p}{m} K_M n_a \quad (2)$$

where higher terms on n_a have been neglected. It can be seen here that as p approaches unity, the system then behaves as if it was comprised of isolated units in a macromolecule and there is no enhanced sensitivity to the quenching. As p approaches m, the system behaves as having an exciton delocalized over the major part of the macromolecule and the increased sensitivity scales with the value of m due to enhanced association constant K_M. This can also relate to the results of ultrafast anisotropy decay. For the case of anisotropy decay between coupled, randomly oriented chromophores in a macromolecule, one finds the residual value is given as[21,22]

$$r_\infty = 0.4/p \quad (3)$$

This or a similar value was often measured in steady-state measurements and used in the estimation of the exciton migration domain.[19,20] Measurements of the time-resolved anisotropy decay are very powerful in probing the ultrafast kinetics observed in the organic macromolecular systems when coupling is relatively strong.[10] This anisotropy decay measurement also allows one to develop a good comparison between the results and conclusions obtained from steady-state measurements with those of more detailed analysis. In our previous investigations we have shown that with steady-state estimates alone one cannot accurately describe either the exciton migration length or the time scale, and this may cause overestimates of the exciton diffusion length. With these ultrafast techniques and with the model above we are looking for a clearer description for the scale of exciton diffusion length in organic macromolecules which are useful for amplified sensing applications.

In this paper we report the use of a specific model and nonlinear and time-resolved measurements for investigating the mechanism of energy migration in amplified fluorescence quenching effects of TNT in a set of organic dendrimers. With these techniques one may describe more closely the limits of exciton migration (and its mechanism) in fluorescence quenching applications for sensing TNT. In our previous publication we found that two-photon fluorescence could be used for sensing TNT with a multichromophore dendritic nanodot used as the substrate;[23] and this contribution is directed toward the analysis of the never-so-important mechanism of enhanced quenching via exciton migration.

2. Experimental Details

Synthesis of Organic Dendrimers. Organic dendrimers with a large two-photon cross section were synthesized by grafting varying numbers of TP-active chromophores to phosphorus dendrimers (G1−G4, Figure 1). The complete synthesis and characterization of the dendrimers were reported previously.[24] Dendrimer generations of G1 to G4 have 12, 24, 48, and 96 chromophores, respectively.[24] They possess high quantum yields

ranging from 0.48 to 0.75, absorb in the 380 nm region, and emit in the 430−500 nm region.[24]

G4 system possesses 96 two-photon absorbing chromophores on the near spherical surface of the dendrimer. These chromophores are quasi-1D quadrupolar systems assembled from the grafting of donor moieties by the use of conjugated spacers onto a fluorenyl core.[24,25] Such chromophores have been reported previously to exhibit large TPA cross-sections per unit,[25] which results in a very high two-photon absorption cross-section per dendrimer macromolecule reaching 55 900 GM for G4.[25]

Steady-State Absorption and Emission. Ultraviolet (UV)−visible absorption spectra were recorded with an Agilent Technologies 8453 spectrophotometer. Steady-state fluorescence measurements were performed on a Fluomax-2 fluorimeter. Both toluene and tetrahydrofuran (THF) were used as solvents for all spectroscopic measurements.

Time-Resolved Fluorescence Spectroscopy. Time-resolved polarized fluorescence measurements were carried out on a femtosecond fluorescence up-conversion setup. A detailed description of the setup has been given elsewhere.[11,12] In brief, the solution was excited with frequency-doubled light from a mode-locked Ti-sapphire laser (Tsunami, Spectra Physics) with a pulse width of ∼100 fs in a wavelength range of 385−430 nm. A Berek compensator was utilized to control the polarization of the excitation beam for fluorescence anisotropy measurement. The sample cell was 1 mm thick and was held in a rotating holder to avoid possible photodegradation and other accumulative effects. The horizontally polarized fluorescence emitted from the sample was up-converted in a nonlinear crystal of β-barium borate. This system acts as an optical gate and enables the fluorescence to be resolved temporally with a time resolution of about 200 fs (fwhm).[11,12] Spectral resolution was achieved by dispersing the up-converted light in a monochromator and detecting it by using a photomultiplier tube (Hamamatsu R1527P).

The fluorescence anisotropy decay was calculated according to the expression:

$$r(t) = \frac{I_{par} - GI_{per}}{I_{par} + 2GI_{per}} \quad (4)$$

Here, I_{par} and I_{per} are the intensities of fluorescence polarized vertically and horizontally to the polarization of excited light, respectively. The G factor accounts for the varying sensitivities for the detection of emission at vertical and horizontal polarization configurations. The G factor was corrected by using standard dye in this experiment.

Fluorescence Quenching Experiment. Fluorescence quenching experiments were carried out by microtitration in solution. The titration procedure involved the placement of a 1.5 mL sample solution in a 0.5 cm Quartz cell. Initially, the fluorescence spectrum was recorded in the absence of a quencher at room temperature with use of the Fluoromax-2 (SPEX) spectrophotometer. To the initial solution, microliter additions of a solution that contained the sample at the same concentration and the quencher at a known concentration were performed, and fluorescence spectra were acquired after each microliter addition. Stern−Volmer plots were made with the acquired data.

3. Results and Discussion

In these experiments we used two different solvents (THF and toluene) to dissolve dendrimers G1 to G4. Optical absorption and fluorescence spectra of the dendrimers in toluene have been published elsewhere.[24] Shown in Figure 2 are the normalized absorption and fluorescence spectra of the dendrimer generations from G1 through G4 in THF.

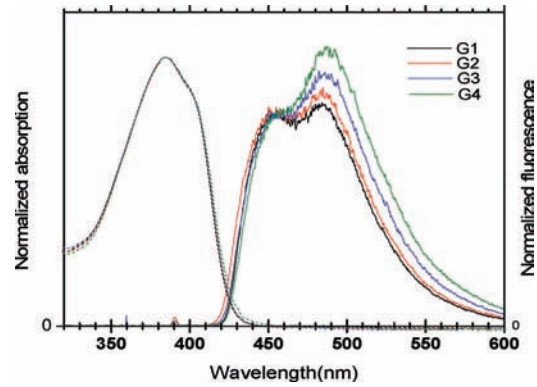

Figure 2. Normalized absorption and steady-state emission spectra (excited at 380 nm) in THF of the dendrimer generations G1−G4 bearing 12, 24, 48, and 96 chromophores, respectively.

The absorption spectrum is nearly independent of the generation number, which indicates the existence of a weak interchromophore coupling in the ground-state configuration.[18,26] At the same time the fluorescence spectra of the dendrimers show dependence on the generation number, which indicates stronger interchromophore interactions in the excited state. This dependence can also be associated with slightly different relaxation configurations for different generations resulting from more densely packed periphery groups for larger dendrimers.[27] Even if the absorption spectra are essentially the same in THF and toluene, the fluorescence spectra in THF slightly deviate from those in toluene and demonstrate increased Stokes shift.[24] This fluorescence dependence on solvent can be rationalized by higher polarity of THF with respect to toluene and the dipolar character of the chromophores.[25]

In our previous work we found that the fluorescence of the dendrimers is sensitive to the presence of TNT.[23] Due to the strong two-photon absorption properties of these dendrimers,[24] the sensors based on the fluorescence quenching can be efficiently activated by the near-infrared light with use of the two-photon absorption route for the excitation.[23] The quenching efficiency can be quantified with the Stern−Volmer relation

$$F_0/F_q = 1 + K_{SV}[M] \quad (5)$$

In this equation, F_0 is the initial fluorescence intensity without quencher, F_q is the fluorescence intensity in the presence of the quencher (TNT) with a concentration [M], and K_{sv} is the Stern−Volmer constant. We have measured the fluorescence quenching efficiency as a function of the dendrimer generation number. The Stern−Volmer (S−V) plots for the lowest and highest generation numbers (G1, G4) are shown in Figure 3.

The Stern−Volmer quenching constant K_{SV} for the G4 dendrimer was found to be ∼1400 M^{-1},[23] which is systematically higher as compared to S−V factors obtained under similar conditions for various amplifying polymers used for TNT detection.[28,29] It is also seen from Figure 3 that the S−V factor as well as quenching efficiency rises with the increase of the generation number. To better understand this encouraging trend in the enhancement of the sensing performance with higher generation dendrimers and the quenching mechanism behind this trend, we have performed detailed investigations on the exciton migration in these dendrimers by means of femtosecond

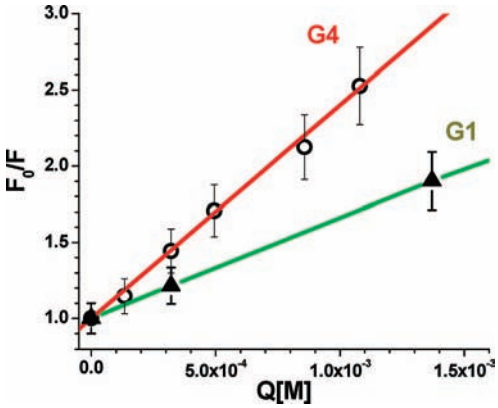

Figure 3. Stern−Volmer plot for the fluorescence quenching of dendrimers with TNT. The comparison of two-photon excited fluorescence quenching (excitation at 800 nm) of dendrimers G1 and G4 by TNT, respectively, is shown. The scattering of the data points characterizing the signal-to-noise ratio of two-photon approach with relatively small average laser intensity of a few milliwatts remains quite small and the dependence obtained by using one-photon excitation is analogous.[23]

time-resolved spectroscopy. In polymer studies[4,6−8,30] as well as in investigations in Langmuir−Blodgett films[19] and nanofibrils,[31] an exciton migration was proposed to explain the high quenching efficiency in these systems. In addition, from previous charge and energy transport studies on dendrimers by our group, it was observed that dendrimers can possess excellent exciton transport properties,[11−13,15] implying the possibility of amplified quenching in these systems. In the dendrimer systems G1−G4 studied here, chromophores are distributed over the near-spherical surface of the dendrimer.[24]

It is seen in Table 1 that the average area per chromophore decreases with generation number, which leads to a more dense packing of the chromophores in higher generations. It also can be seen in a way that the distance between chromophores becomes shorter with increasing generation. It is well-known that for the Förster energy transfer mechanism associated with Coulombic interchromophore interaction, the transfer rate is inversely proportional to the sixth power of the distance d between chromophores.[32] To illustrate the scaling of the possible Förster-type interchromophore energy transfer rate with the size of the dendrimer, the parameter d^6 is shown in Table 1. Also shown in the table is the two-photon absorption cross-section (σ_2), which is impressive for all and in particular for the dendrimer generation G4. It was mentioned above that the steady-state one-photon absorption spectra (Figure 2) showed no dependence on generation number, which indicates weak interaction between chromophores in the absorption configuration. Two-photon cross section increases nearly linearly with the number of chromophores further supporting the idea of a relatively weak interchromophore coupling regime in these systems. Time-resolved spectroscopy methods such as time-resolved fluorescence anisotropy allow one to follow exciton migration over the surface and directly connect it to the quenching dynamics and nonlinear properties.[10]

Femtosecond Time-Resolved Fluorescence. The time-resolved fluorescence intensity decay taken at the magic angle of the polarizer is shown in Figure 4. Fluorescence decay has been detected at 470 nm.

With fitting these decay curves it was found that a decay component in a time scale of ∼70 ps is present for all three different generations along with the long component of 700 ps. No substantial contribution of the dynamics faster than 70 ps has been measured except for a small detection-wavelength-dependent solvation component (∼1 ps). The long time component of the fluorescence decay (∼700 ps) was previously accurately measured by using time-correlated single-photon counting and found to be near independent of the dendrimer size.[24] We have fitted the isotropic fluorescence profile to a two-exponential decay function keeping the long decay time fixed at 700 ps. The results are listed in Table 2.

It is seen from the table that the contribution of the ∼70 ps component increases with the increase of the dendrimer size. This finding may help to rationalize the decrease of quantum yield at higher generation dendrimers reported earlier (0.48 for G4 vs. 0.71 for G2).[24] As the contribution of the fast decaying fluorescence to the time-integrated fluorescence is very small, the quantum yield should be proportional to the relative contribution of the long 700-ps component. The ratio of amplitudes for G2 and G4 is $(A_2)_{G2}/(A_2)_{G4} = 1.40$ while the ratio of quantum yields is $(QY_{G2})/(QY_{G4}) = 1.47$.[24] These numbers are in a good agreement taking into account the simplified model used for the interpretation. Furthermore, the ∼70-ps time component can be correlated to the average time for the exciton to reach the intrinsic quenching site (defect) in the system. The relatively long time lag of 70 ps between the excitation and quenching by intrinsic defects allows the exciton with a short hopping time of ∼1 ps (see below) to perform multiple hops between chromophores, thus covering substantial area on the surface of the dendrimer. However, the intrinsic quenching originated from defects remains small in the G4 dendrimer, as its quantum yield is still relatively high at ∼48%.

Time-Resolved Fluorescence Anisotropy. The anisotropy decay is utilized to monitor the exciton migration over the dendrimer spherical surface. For different orientations of the chromophores, each interchromophore exciton migration step leads to the reorientation of the emitting dipole and results in fluorescence depolarization.[1,22] The fluorescence depolarization dynamics can be followed by means of the time-resolved spectroscopy and connected in this case to the exciton migration parameters.[15,21,22] While this approach is more or less straightforward for randomly oriented chromophores or for the morphologies possessing well-defined angular distributions, it is difficult to apply this approach to near-linear systems similar to polymers. In an ideal polymer the transition moment is not supposed to change orientation in the course of the exciton migration along the linear chain, leaving the fluorescence polarized and not sensitive to exciton migration. In organic polymers due to imperfections in the chain (kinks, other defects) and interchain energy transfer, emission dipole does change orientation and fluorescence anisotropy decays to some residual value.[33,34] However, the particular geometry and the mutual chain arrangements are not well-known, making it very difficult to connect the fluorescence anisotropy to the exciton path and exciton migration length. Dendrimers are known to possess much more ordered organization of building blocks with defined geometry and different orientations.[35,36] This constitutes a fundamental advantage of the dendrimers in terms of our ability to follow important exciton migration parameters, such as delocalization length, interchromophore coupling strength, and hopping range by means of fluorescence anisotropy.[10−15,21]

Anisotropy decay results for the dendrimer system G3 on different time scales are shown in Figures 5 and 6. Fluorescence was excited at 400 nm. The experimental fluorescence anisotropy $R(t)$ was calculated from the decay curves for the intensities of fluorescence polarized parallel $I_{par}(t)$ and perpendicular $I_{per}(t)$ to the polarization of the excitation light according to eq 4. The

TABLE 1: Geometrical Parameters and Two-Photon Responses of the Dendrimers G1−G4

dendrimer generation	diameter (nm)	surface area (nm^2)	no. of chromophores	surface area per chromophore (nm^2)	av distance d between chromophores (nm)	d^{6a} (nm^6)	σ_2 at λ_{TPA}(max) (GM^b)[22]
G1	4.79	72.04	12	6.00	2.45	216.00	8880
G2	6.74	142.64	24	5.94	2.44	209.58	17700
G3	8.66	235.48	48	4.90	2.21	117.65	29800
G4	10.60	352.8	96	3.675	1.92	49.63	55900

[a] d^6 is inversely proportional to the Förster energy transfer time (hopping time) between chromophores. [b] σ_2 is the two-photon absorption cross-section. 1 GM = 10^{-50} cm^4 s $photon^{-1}$.

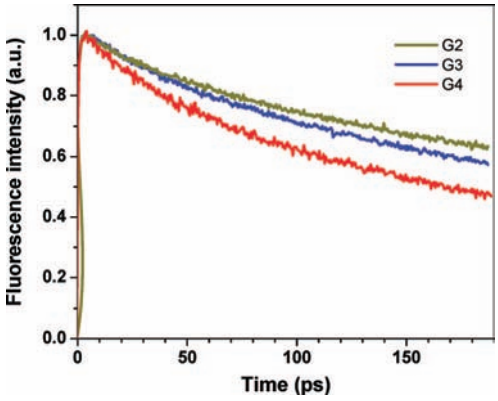

Figure 4. Normalized time dependent fluorescence decay of the dendrimer generations from 2 to 4 (G2 to G4) in THF solution. Excitation wavelength is 400 nm, detection wavelength is 470 nm.

TABLE 2: Time Components and Their Amplitudes for the Fluorescence Up-Conversion Results at the Excitation of 400 nm for the Dendrimer THF Solutions

	t_1 (ps)	A_1	t_2 (ps)	A_2
G1	66	0.079	700	0.921
G2	65	0.198	700	0.802
G3	80	0.287	700	0.713
G4	77	0.426	700	0.574

factor G accounts for the difference in sensitivities for the detection of emission in the perpendicular and parallel polarized configurations. Starting from anisotropy close to ~0.4, the anisotropy decays to near zero on a time scale of ~100 ps. Taking into account the very large size of G3 and the viscosity of toluene (~0.56 cP at 25 °C), the longest time decay component in G3 anisotropy is not associated with the overall molecular rotation (rotational diffusion) of G3 in toluene. Interdendrimer energy transfer also can be ruled out because at the concentration used in this experiment (ca. $10^{-5}-10^{-4}$ M), the average intermolecular distance is about 50 nm while the Förster radius for the energy transfer can be estimated to be a few nanometers. This combination of parameters (including G3 fluorescence lifetime of ~700 ps[24]) leads to intermolecular energy transfer time on a submillisecond time scale. Therefore we should assign the transition dipole reorientation to the intramolecular (intradendrimer) process and it is due to the exciton migration over the surface.

As seen from Figure 5 fluorescence anisotropy decays to near zero after 200 ps. Taking into account the experimental error, the anisotropy value in this area (>200 ps) should not exceed 0.02. For randomly oriented chromophores this implies migration (equilibration) over ~20 chromophores (eq 3).

In the case of regular organization of chromophores at a fixed angle with respect to the surface, the change of the emission dipole can be roughly correlated to the position on the surface. A simple equation for the fluorescence anisotropy in the case of hindered rotation (in our case this means averaging over the

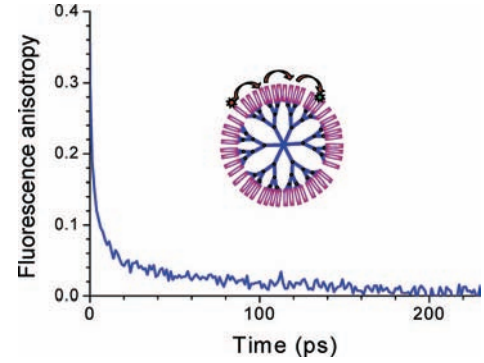

Figure 5. A schematic description of the time-dependent fluorescence anisotropy decay of dendrimer G3 in toluene due to exciton migration along the dendrimer surface.

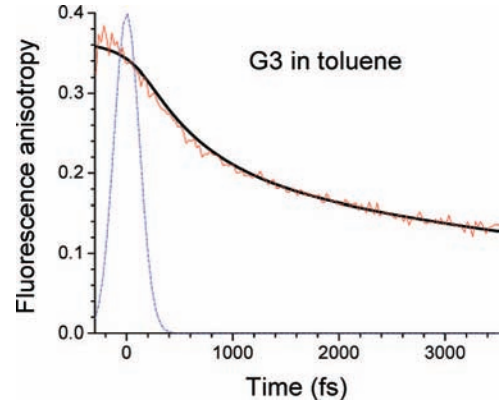

Figure 6. Short time scale of time-resolved fluorescence anisotropy of dendrimer G3 in toluene with instrument response function IRF (blue dotted line). Excitation wavelength is 400 nm, detection wavelength is 480 nm. The dark solid line is the result from best fit modeling.

angles within the cone of accessible dipole orientations) can be used:[32]

$$r = 0.4\left[\frac{1}{2}(\cos\theta_C)(1 + \cos\theta_C)\right]^2 \quad (6)$$

where θ_C is the cone angle, and the range of θ_C can be estimated in course of the exciton migration from the anisotropy r. This simple estimation gives the angle $\theta_C = 69°$, which corresponds to 32% of sphere's surface to be covered by exciton. The number of chromophores on this spherical segment is ≃16 for G3. This gives us an estimation of the number of chromophores covered by exciton migration in the limiting case of regular organization of the chromophores at a fixed angle with respect to the dendrimer surface.

Fluorescence anisotropy decay on a short time scale is shown in Figure 6. The raw fluorescence anisotropy decays from an initial value of ~0.34 at time zero to the anisotropy of ~0.14 at a time of 3 ps. In case of fast dynamics, the measured profiles

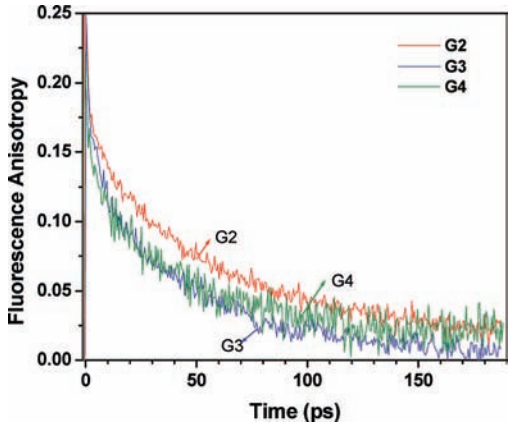

Figure 7. Comparison of the intermediate time scale of time-resolved fluorescence anisotropy of different dendrimer generations G2 (red), G3 (blue), and G4 (cyan) in THF solution. Excitation wavelength is 400 nm.

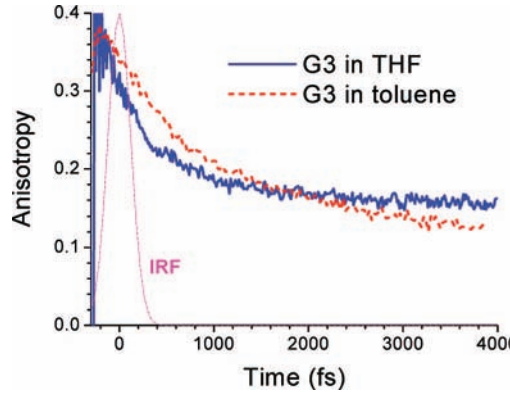

Figure 8. The solent effect (THF and toluene) on the time-resolved fluorescence anisotropy of the dendrimer G3 on a short time scale. Instrument response function (IRF) is also shown (dash-dot line).

$I_{par}(t)$ and $I_{per}(t)$ are the results of a convolution of the instrument response function with true fluorescence intensity profiles. In this case the raw anisotropy looks different from the true anisotropy profile at short times and its peak appears at negative times. Parameters of true anisotropy decay can be estimated by best fit procedures assuming the convolution of the instrument response function (IRF) with model parallel and perpendicular fluorescence intensity profiles.[37,38] The best fit to a two-exponential anisotropy decay model is shown in Figure 6 by the solid line. The best fit anisotropy was found to decay from initial value of 0.40 ± 0.03 within the time constant of 575 ± 20 fs.

This time constant is relatively long as compared to some other strongly interacting dendrimer systems,[10,11,13] which may indicate the incoherent hopping exciton transport in this system.[15] The fast decay component is generation dependent and fluorescence anisotropy decays much faster in a higher generation dendrimer, as the dendrimer becomes more densely packed and the distance between chromophore shortens (see discussion below). The fluorescence anisotropy decay curves of different dendrimer generations (G2 to G4) on a long time scale are plotted in Figure 7.

It is seen that the anisotropy decay on this time scale weakly depends on dendrimer generation. While the decay profiles for G3 and G4 are the same within experimental error, the anisotropy for G2 decays slightly slower. This slower decay can be associated with less densely packed chromophores for smaller generation dendrimers. The shorter time components in anisotropy decay showed the same decreasing trend with the increase of generation number (see Figure 11a and discussion below).

To gain an insight into the molecule architectural effect, we investigate the behavior of fluorescence anisotropy decay in different polarity solvents (THF and toluene) for dendrimer generation from G1 to G4. The anisotropy decay in varying solvents can provide information on the details of the arrangement and interaction between the chromophores in different solvents.

On the basis of our investigation, the different generation of dendrimers G1, G2, G3, and G4 display the same trend regarding the anisotropy decay behavior in these two solvents. Figure 8 shows an example of the fluorescence anisotropy profiles for dendrimer G3 in THF and in toluene. In general the G3 anisotropy decay in both solvents (THF and toluene) can be approximated by a two-exponential decay function on this time scale. A fast initial decay on the time scale of hundreds of femtoseconds gives way to a slower decay in the picosecond time scale. It is seen from Figure 8 that in a more polar solvent of THF (polarity index of 4), the first decay component ($\tau_s \simeq 180$ fs) is shorter than that in toluene (polarity index of 2.4) with the fast decay component of $\tau_s \simeq 575$ fs (derived from more accurate fitting with IRF convolution compared to the value published[23]). Opposite to the trend in short components the second decay component in THF is longer compared to that in toluene (Figure 8). More polar solvent THF can facilitate the chromophore aggregation on the dendrimer's surface, especially at higher generations where the increasing packing density and strong interchromophore interactions can favor the self-organization process.[39] The deviation of the decay behavior in two different solvents may be rationalized in terms of the degree of clusterization (surface aggregate formation), that is to say, in a more polar solvent (THF in this case), the inhomogeneous distribution of chromophores on the dendrimer surface will result in multiexponential anisotropy decay profile. The first decay component in this case may be related to the intracluster relaxation; it becomes faster due to the increased aggregation and the decreased distance between chromophores inside surface chromophore aggregates in THF. The longer decay component reflects the intercluster hopping rate, which is reasonable to be slower for higher generations due to the formation of more isolated surface aggregates. Two-component anisotropy decay due to clusterization within the photosynthetic antenna has been reported by Prof. Fleming and co-workers.[40] Our anisotropy data also indicate the distribution of chromophore on the dendrimer surface to be more uniform in a less polar solvent (toluene). If we go back to the anisotropy decay in toluene, the absence of the ultrafast dynamics (<500 fs) points to an incoherent hopping regime for exciton migration over the dendrimer surface. Weak clusterization and inhomogeneous distribution of the chromophores on the surface can lead to some distribution of the hopping times in toluene solution too. The shortest time components in anisotropy decay may reflect the fastest hopping rates in the systems. The average hopping rate can be estimated from the e-times drop in fluorescence anisotropy decay which occurs at ~3 ps. This time scale can be compared to the decay process responsible for fluorescence quenching on intrinsic defects (~70 ps) described above. The comparison suggests that exciton is able to perform ~23 hops before being quenched by intrinsic defect. This estimation based on the comparison of the fluorescence and fluorescence anisotropy decay times is in good agreement with that made above on the basis of the residual anisotropy analysis. These results

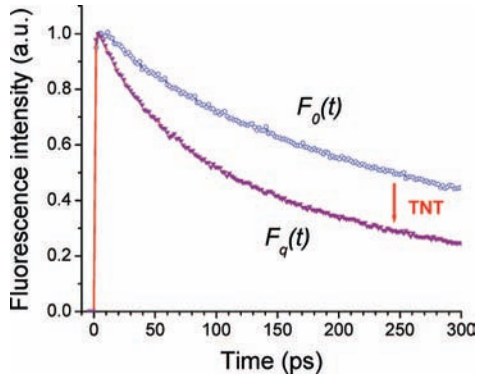

Figure 9. Difference in fluorescence dynamics between the pure dendrimer G3 solution (open circles) and the solution after exposure to TNT (filled triangles). Excitation wavelength is 400 nm, detection wavelength is 480 nm.

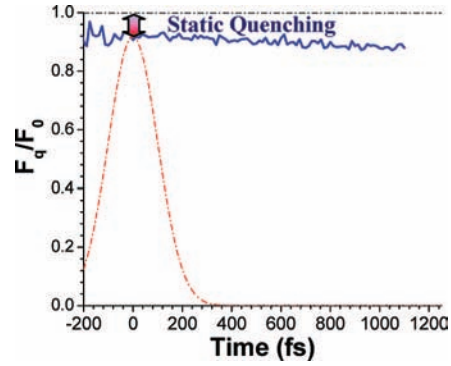

Figure 10. Quenching ratio F_q/F_0 as a function of time on a short time scale. It shows a fractional static contribution to the fluorescence quenching.

undoubtedly demonstrate the multistep exciton migration process that produces a long exciton diffusion domain over the dendrimer surface beneficial for the efficient amplified quenching of the explosives, such as TNT.

Quenching Dynamics and Its Connection to the Exciton Transport. Figure 9 schematically displays the difference between fluorescence dynamics for dendrimer sample with TNT (concentration: 5×10^{-3} M) $F_q(t)$ and that for pure dendrimer solution $F_0(t)$.

It is seen that the fluorescence from the sample with quencher (TNT) decays faster than that without quencher, which reflects the substantial rise of the number of quenched excitons on the picosecond time scale. It is worth noting that the difference in the decay profiles saturates roughly at the same time scale as that at which fluorescence anisotropy completely decays (see Figures 5 and 7). The quenching ratio $Q(t) = F_q(t)/F_0(t)$ represents the fraction of quenched excitations at a given delay time t. The time-resolved quenching ratio $Q(t)$ on a short time scale is shown in Figure 10. It is seen from this figure that ~10% of fluorescence is quenched within the time resolution of the up-conversion setup. Taking into account the absence of any measurable fast dynamics for $Q(t)$ in the vicinity of instrument response function, this fraction of quenching can be considered as instantaneous or true static, and related to the excitation photons being absorbed on nonemissive sites. This is different from the quenching dynamics in conjugated polyelectrolyte where the fast time component has been detected for $Q(t)$ in time-resolved experiments.[30] In our experiments the fastest time component in the quenching ratio decay is ~1.5 ps. This is close to the ~0.58 ps fast time component found in anisotropy experiments (Figure 6). Both time constants represent the hopping time between adjacent chromophores by order of magnitude while exact expressions for the anisotropy and for the exciton trapping time can be different.[21,22,41] The major part of the fluorescence quenching by TNT occurs on the time scale of ~150 ps (Figure 9) and should be considered as a dynamic quenching. The fluorescence anisotropy which reflects the exciton migration over the chromophores on the dendrimer surface also decays to zero around 150 ps. This directly connects the exciton migration over the surface of the dendrimer to the dynamic quenching proving the crucial role of exciton migration in the enhanced fluorescence quenching in dendrimer macromolecules.

It is also seen from Figures 9 and 10 that both static and dynamic quenching components take account together for the fluorescence quenching by ~50% at long delays, which is in excellent agreement with steady-state measurements which showed the same total amount of quenching at this TNT concentration.

Simple estimation of the TNT diffusion-controlled quenching at the quencher concentration of 10^{-3} M gives the maximum value of collision time of about 100 ns, [32] whereas the experimental time scale of the dynamic quenching is in the picosecond range from time-resolved measurement studies. Comparison of time integrated fluorescence quenching with the dynamic drop in fluorescence (Figure 9) proves that in our case the contribution from the dynamic quenching associated with the diffusion of TNT in solution is negligible. For this case the fluorescence quenching is in major part a fast dynamic process on a picosecond time scale, which results from the fast exciton migration on the dendrimer surface from the initially excited site to the site associated with the TNT−chromophore complex.

To obtain further insight into the quenching mechanism, we compared the quenching dynamics for different generations of the dendrimers. As we mentioned above (Figure 3) the quenching performance is better for higher generation dendrimers. Panels a and b of Figure 11 show time-resolved fluorescence anisotropies for the dendrimers G1 and G3, respectively. It is seen from Figure 11a that the initial anisotropy decay rate is faster for G3 as compared to G1. Best fit analysis which included convolution with instrument response function revealed fast components of 0.992 and 0.575 ps for G1 and G3, respectively. The initial anisotropy decay rate is directed by the hopping rate between the chromophores on the dendrimer surface indicating that the hopping rate is higher for G3. Overall anisotropy decay for G3 remains faster for G3 on the longer time scale (Figure 11b) as well.

The ratio of hopping rates in G3 and G1 (0.992/0.575 = 1.73) is in good agreement with the ratio of Förster transfer rates estimated from geometrical parameters listed in the Table 1: $r_{G3}^6/r_{G1}^6 = 216.0/117.7 = 1.83$. This clearly indicates that the faster exciton migration rate in G3 results from more dense packing and smaller interchromophore separation on the surface of higher generation dendrimers. The quenching ratio F_q/F_0 dynamics of G1 and G3 for the same TNT quencher concentration is shown in Figure 11c. It is clearly seen from this figure that the fraction of quenched chromophores increases faster for higher generation dendrimer G3. This is the direct consequence of the higher interchromophore hopping rate in G3 detected by fluorescence anisotropy measurements. The higher hopping rate in G3 as compared to G1 facilitates a larger exciton migration domain in G3. The larger number of chromophores covered by the exciton migration results in the better sensing performance for larger dendrimers found in simple model calculations (eq 2) and in our experiments (Figure 3). Comparing the Stern−

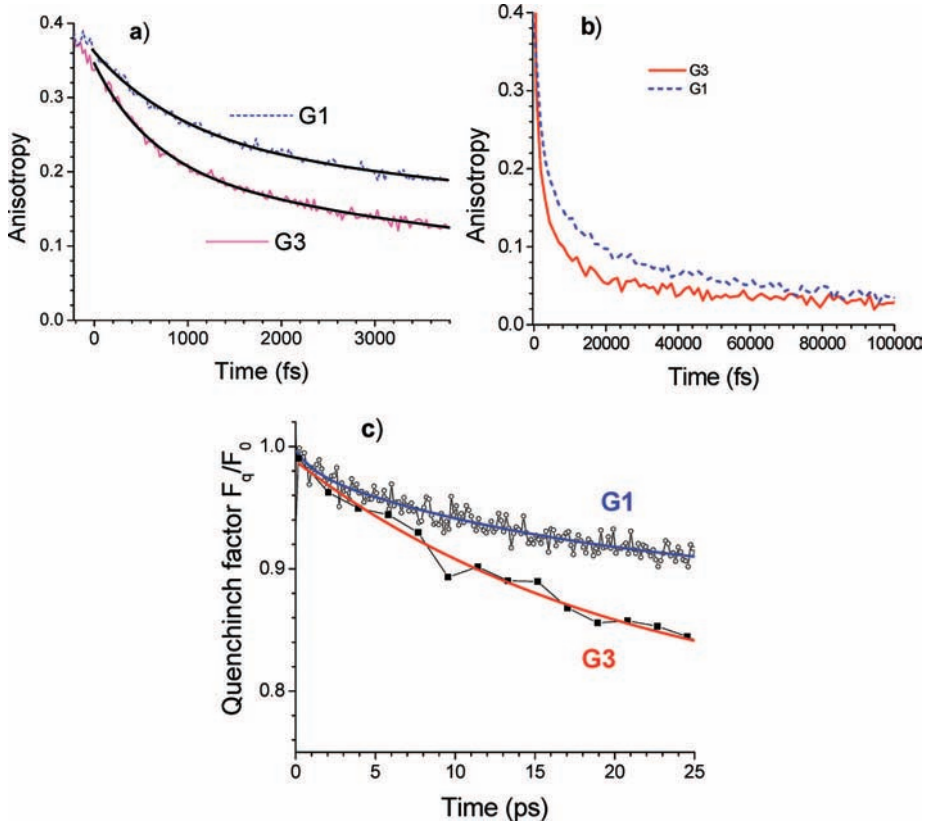

Figure 11. Fluorescence anisotropy decay of dendrimers in short time scale (a), long time scale (b), and the quenching dynamics (c) for dendrimers G1 and G3, respectively.

Volmer factor obtained for the G4 dendrimer in solution (~1400 M^{-1})[23] with those obtained under similar conditions for the various amplifying polymers used for TNT detection,[28] one can see that the dendrimer's S−V factor K_{SV} is systematically higher. This can be associated with the system's architecture. In polymers the exciton transport is supposed to be mostly one dimensional ("molecular wire" approach),[7] while in large dendrimers the exciton transports over the near-spherical surface, i.e., quasi-two-dimensional. It was shown by Montroll[41] that the number of steps $\langle n \rangle$ required by the exciton to reach a trapping center scales differently with the relative concentration of trapping centers. In particular $\langle n \rangle \approx N^2$ in the one-dimensional case, while $\langle n \rangle \approx N \log N$ in the two-dimensional system (N is the number of chromophores per one trapping (quenching) center).[41] It is seen that for the same low quencher concentration (large N), the number of steps required for exciton to reach quencher in the two-dimensional system is smaller than that for the one-dimensional system. This means that the number of hopping steps required for exciton to reach the quenching site is smaller for the quasi-two-dimensional dendrimer surface as compared to the linear polymer. This may contribute to the enhanced sensing response of the dendrimers relative to polymers.

4. Conclusions

We have investigated the exciton dynamics in new dendritic materials which are promising two-photon sensors for TNT detection. These materials possess the exceptional combination of large δ_{TPA} with efficient amplified fluorescence quenching by TNT. We have directly connected fluorescence time-resolved anisotropy measurements with that of the excitation migrating over the dendrimer surface to the quenching site. Our investigation showed that this exciton migration over many units to the TNT−dendrimer complex sites plays a dominant role in the fluorescence quenching process. The time components describing the exciton migration over the dendrimer surface are in the same range as those observed for the dynamic quenching, thus proving that the exciton migration over the dendrimer surface is the main contributor to the observed dynamic fluorescence quenching. This validates the efficient amplified quenching mechanism associated with exciton migration over the dendrimer surface as a main quenching mechanism. Our results also indicate that the migration over the quasi-two-dimensional dendrimer surface results in more efficient amplified quenching than that along the one-dimensional polymer chains ("molecular wires").

Acknowledgment. We thank the National Science Foundation (polymers) for support of this research.

Supporting Information Available: Details of the estimation of the fluorescence quenching in the presence of the exciton migration. This material is available free of charge via the Internet at http://pubs.acs.org.

References and Notes

(1) Scholes, G. D.; Rumbles, G. *Nat. Mater.* **2006**, *5*, 683–696.
(2) Blankenship, R. E. *Molecular Mechanisms of Photosynthesis*; Blackwell Science: Oxford, UK, 2002.
(3) Bar-Haim, A.; Klafter, J.; Kopelman, R. *J. Am. Chem. Soc.* **1997**, *119*, 6197–6198.
(4) Yang, J.-S.; Swager, T. M. *J. Am. Chem. Soc.* **1998**, *120*, 11864–11873.
(5) Cumming, C. J.; Aker, C.; Fisher, M.; Fox, M.; La Grone, M. J.; Reust, D.; Rockley, M. G.; Swager, T. M.; Towers, E.; Williams, V. *IEEE Trans. Geosci. Remote Sensing* **2001**, *39*, 1119–1128.
(6) Thomas, S. W., III.; Joly, G. D.; Swager, T. M. *Chem. Rev.* **2007**, *107*, 1339–1386.
(7) Swager, T. M. *Acc. Chem. Res.* **1998**, *31*, 201–207.

(8) Yang, J.-S.; Swager, T. M. *J. Am. Chem. Soc.* **1998**, *120*, 5321–5322.
(9) Poliakov, E. Y.; Chernyak, V.; Tretiak, S.; Mukamel, S. *J. Chem. Phys.* **1999**, *110*, 8161–8175.
(10) Goodson, T., III. *Acc. Chem. Res.* **2005**, *38*, 99–107.
(11) Varnavski, O.; Yan, X.; Mongin, O.; Blanchard-Desce, M.; Goodson, T., III. *J. Phys. Chem. C* **2007**, *111*, 149–162.
(12) Varnavski, O.; Samuel, I. D. W.; Pålsson, L.-O.; Beavington, R.; Burn, P. L.; Goodson, T., III. *J. Chem. Phys.* **2002**, *116*, 8893–8903.
(13) Ranasinghe, M. I.; Varnavski, O.; Pawlas, J.; Hauck, S. I.; Louie, J.; Hartwig, J. F.; Goodson, T., III. *J. Am. Chem. Soc.* **2002**, *124*, 6520–6521.
(14) Varnavski, O.; Menkir, G.; Goodson, T., III.; Burn, P. L. **2000**, *77*, 1120−1122.
(15) Varnavski, O.; Ostrowski, J. C.; Sukhomlinova, L.; Tweig, R. J.; Bazan, G. C.; Goodson, T., III. *J. Am. Chem. Soc.* **2002**, *124*, 1736–1743.
(16) Ramakrishna, G.; Bhaskar, A.; Bauerle, P.; Goodson, T., III. *J. Phys. Chem. A* **2008**, *112* (10), 2018–2026.
(17) Wu, C.; Malinin, S. V.; Tretiak, S.; Chernyak, V. Y. *Nature Phys.* **2006**, *2*, 631–635.
(18) Thompson, A. L.; Gaab, K. M.; Xu, J.; Bardeen, C. J.; Martinez, T. J. *J. Phys. Chem. A* **2004**, *108*, 671–682.
(19) Levitsky, I. A.; Kim, J. S.; Swager, T. M. *J. Am. Chem. Soc.* **2004**, *126*, 452–453.
(20) Rose, A.; Tovat, J. D.; Yamaguchi, S.; Nesterov, E. E.; Zhu, Z.; Swager, T. M. *Philos. Trans. R. Soc. London, Ser. A* **2007**, *365*, 1589–1606.
(21) Yeow, E. K. L.; Ghiggino, K. P.; Reek, J. N. H.; Crossley, M. J.; Bosman, A. W.; Schenning, A. P. H. J.; Meijer, E. W. *J. Phys. Chem. B* **2004**, *104*, 2596–2606.
(22) Finger, K. U.; Marcus, A. H.; Fayer, M. D. *J. Chem. Phys.* **1994**, *100*, 271–286.
(23) Narayanan, A.; Varnavski, O.; Mongin, O.; Majoral, J. P.; Blanchard-Desce, M.; Goodson, T., III. *Nanotechnology* **2008**, *19*, 115502.
(24) Mongin, O.; Krishna, T. R.; Werts, M. H. V.; Caminade, A. M.; Majoral, J. P.; Blanchard-Desce, M. *Chem.Commun.* **2006**, 915–917.
(25) Mongin, O.; Porrès, L.; Moreaux, L.; Mertz, J.; Blanchard-Desce, M. *Org. Lett.* **2002**, *4*, 719–722.
(26) Kopelman, R.; Shortreed, M.; Shi, Z.-Y.; Tan, W.; Xu, Z.; Moore, J. S.; Bar-Haim, A.; Klafter, J. *Phys. Rev. Lett.* **1997**, *78*, 1239–1242.
(27) Bosman, A. W.; Janssen, H. M.; Meijer, E. W. *Chem. Rev.* **1999**, *99*, 1665–1688.
(28) Zhao, D.; Swager, T. M. *Macromolecules* **2005**, *38*, 9377–9384.
(29) Kim, Y.; Zhu, Z.; Swager, T. M. *J. Am. Chem. Soc.* **2004**, *126*, 452–453.
(30) Müller, J. G.; Atas, E.; Tan, C.; Schanze, K. S.; Kleiman, V. D. *J. Am. Chem. Soc.* **2006**, *128*, 4007–4016.
(31) Naddo, T.; Che, Y.; Zhang, W.; Balakrishnan, K.; Yang, X.; Yen, M.; Zhao, J.; Moore, J. S.; Zang, L. *J. Am. Chem. Soc.* **2007**, *129*, 6978–6979.
(32) Lakowicz, J. *Principles of fluorescence spectrocopy*; Kluwer Academic/Plenum Publishers: New York, 2006.
(33) Kim, Y. R.; Lee, M.; Thorne, J. R. G.; Hochstrasser, R. M.; Zeigler, J. M. *Chem. Phys. Lett.* **1988**, *145*, 75–80.
(34) Grage, M. M.-L.; Wood, P. W.; Ruseckas, A.; Pullerits, T.; Mitchell, W.; Burn, P. L.; Samuel, I. D. W.; Sundström, V. *J. Chem. Phys.* **2003**, *118*, 7644–7650.
(35) Fréchet, J. M. J.; Tomalia, D. *Dendrimers and Other Dendritic Polymers*; Wiley: Chichester, UK, 2001.
(36) Newkome, G. R.; Moorefield, C. N.; Vögtle, F. *Dendritic Molecules: Concepts, Synthesis, Perspectives*; Wiley-VCH: Weinheim, Germany, 2001.
(37) Soutar, I.; Swanson, L.; Christensen, R. L.; Drake, R.; Phillips, D. *Macromolecules* **1996**, *29*, 4931.
(38) Cross, A. J.; Fleming, G. R. *Biophys. J.* **1984**, *46*, 45–56.
(39) Wang, B.-B.; Zhang, X.; Jia, X.-R.; Luo, Y.-F.; Sun, Z.; Yang, L.; Ji, Y.; Wei, Y. *Polymer* **2004**, *45*, 8395–8402.
(40) Bradforth, S. E.; Jimenez, R.; van Mourik, F.; van Grondelle, R.; Fleming, G. R. *J. Phys. Chem.* **1995**, *99*, 16179–16191.
(41) Montroll, E. W. *J. Math. Phys.* **1969**, *10*, 753–765.

JP8112123